

Eco-evolutionary diversification of trait convergence and complementarity in mutualistic networks

Francisco Encinas-Viso^{1*}, Rampal S. Etienne^{2**} and Carlos J. Melián^{3**}

1) NRCA & Centre for Australian National Biodiversity Research, CSIRO, GPO Box 1600
Canberra , Australia

2) Groningen Institute for Evolutionary Life Sciences, University of Groningen, The Netherlands

3) Department of Fish Ecology and Evolution, Center for Ecology, Evolution and Biogeochemistry,
EAWAG, Swiss Federal Institute of Aquatic Science and Technology, Switzerland

Keywords: Diffuse coevolution, specialization, sexual reproduction, assortative mating, genetic incompatibilities, dispersal limitation, phylogenetic relatedness, obligate mutualism, morphological constraints, individual based model.

Type of Article: Letters

Number of figures: 6 (5 in color); Number of tables: 2

* Corresponding author: franencinas@gmail.com

** Joint last authorship

1 Empirical plant-animal mutualistic networks show high levels of trait convergence and
2 complementarity, which has been attributed to the action of coevolutionary dynamics
3 between plants and animals. However, some studies suggest that non-selective causes
4 (Brownian trait evolution) may also produce evolutionary trait convergence and comple-
5 mentarity. Furthermore, we do not know the influence of other non-selective factors, such
6 as demographic stochasticity, dispersal limitation and diversification, on quantitative trait
7 divergence and convergence dynamics. Here we present a spatially explicit neutral model
8 of ecological and evolutionary processes based on explicit genetics and quantitative traits
9 to study trait complementarity and convergence in species-rich mutualistic networks, and
10 the emergence of network structure. We also tested our model predictions of convergence
11 and complementarity using an empirical data of a plant-hummingbird community. We
12 find that population and diversification dynamics produce a gradient of species pheno-
13 types ranging from common plant and animal species with large trait variation to rare
14 species with small trait variation that show convergence and complementarity together
15 with high levels of nestedness. More importantly, our results show that our predicted val-
16 ues of convergence are very close to those observed in real communities of pollinators, but
17 not in plants. This suggests that, in contrast to previous models based on coevolutionary
18 selection, ecological (demography and dispersal limitation), genetic (mutation, recomb-
19 nation and assortative mating) and morphological constraints can reproduce some key
20 evolutionary patterns and topological properties of mutualistic networks.

21 Introduction

22 Since Darwin’s book “On The Origin of Species” (Darwin, 1859), the idea of coevolution, defined as
23 reciprocal evolutionary trait change between species, has sparked interest from biologists trying to
24 understand how species interactions generate trait changes. The first clear indication of coevolution
25 was Darwin’s moth example (Darwin, 1862) showing that the long corolla from the orchid *Angraecum*
26 *sesquipedale* could only be reached by a pollinator species with a similar or larger proboscis length.
27 Following the moth and orchid mutualism model system, several studies have modeled coevolutionary
28 dynamics of a few species (Ferriere *et al.*, 2007; Law *et al.*, 2001; Ferdy *et al.*, 2002; Gomulkiewicz
29 *et al.*, 2003; Jones *et al.*, 2009), particularly highly specialized (i.e. obligatory mutualists) systems of
30 plant-animal interactions, such as the fig-fig wasp mutualism (Bronstein *et al.*, 2006). These studies
31 have determined the ecological conditions for coevolutionary stable systems in highly specialized
32 plant-animal interactions (i.e. coESS) (Law *et al.*, 2001; Jones *et al.*, 2009).

33 Janzen (1980) argued that high specialization between plants and animals was not the only example
34 of coevolution, but coevolution can also be the product of multiple-species interactions, a term that
35 he coined “diffuse coevolution”. Diffuse coevolution means that selection on traits is determined
36 by the interaction of more than two species and not only based on pairwise interactions. This is
37 based on the idea of pollination or dispersal “syndromes”, where plants have a set of traits that
38 attract a specific group of pollinator or animal seed-disperser species with traits complementary to
39 those of the plants. The idea of “diffuse coevolution” is thus linked to concepts of complementarity
40 and convergence, and has also been related to patterns of nestedness detected across biogeographic
41 regions in mutualistic networks. We discuss these three important concepts in order.

42 Nestedness, defined as a non-random pattern of interactions where specialist species interact with
43 proper subsets of more generalist species introduces the concept of “diffuse coevolution” in a more
44 quantitative context (Bascompte *et al.*, 2003). Patterns of nestedness have been shown to provide
45 information about the underlying network dynamics. For example, nestedness may be associated
46 with stability and coexistence of species in mutualistic networks (Bastolla *et al.*, 2009; Okuyama
47 & Holland, 2008), although these properties might be also independent of nestedness (Pitchford &
48 Plank 2012).

49 Complementarity, trait matching between mutualistic partners (e.g. corolla length-proboscis length,

50 frugivore body mass-seed size) (Bascompte & Jordano, 2007) could be the product of reciprocal evo-
51 lution (i.e. coevolution). In highly specialized two-species interactions, as for example the fig-fig wasp
52 mutualism (Bronstein *et al.*, 2006), plants coevolve with their most efficient pollinator to strengthen
53 the complementarity of their matching adaptations (i.e., coevolutionary selection). There are also
54 situations where an insect will be unable to reach nectar in floral tubes longer than its proboscis:
55 the tube length sets up a barrier to some species, but not to others. For example, combining rules
56 that link plants to pollinators whose trait ranges overlap and rules that link pollinators to flowers
57 whose traits are below a pollinator-specific barrier value seem to predict structural properties of
58 empirical mutualistic networks (Santamaría & Rodríguez-Gironés, 2007). Thus, developmental and
59 morphological constraints may be required to explain complementarity (Bascompte & Jordano, 2007;
60 Anderson *et al.*, 2010).

61 Convergence, the independent evolution of similar features in the same community in different
62 evolutionary lineages is a common, perhaps a ubiquitous phenomenon but its interpretation is not
63 clear-cut (Losos, 2011). Selective and non-selective causes can produce evolutionary trait conver-
64 gence (Losos, 2011). Traits may evolve according to the same environmental or biotic pressures in
65 independent lineages or as Brownian motion with speciation occurring randomly (Stayton, 2008).
66 Evolutionary convergence in plant-animal mutualisms partly explains the formation of 'syndromes'
67 produced by the presence of specific mutualist partner species (Waser *et al.*, 1996; Howe & Small-
68 wood, 1982; Bascompte & Jordano, 2007). For example, plant species with a specific corolla mor-
69 phology may determine the evolutionary convergence of pollinator species traits (Jousselin *et al.*,
70 2003; Guimarães *et al.*, 2011).

71 Ecological models have mostly focused on population dynamics to study nestedness while evolution-
72 ary models have focused on trait-based dynamics of interacting species, particularly the emergence
73 of complementarity and convergence in the absence of population dynamics (Nuismer & Doebeli,
74 2004; Kokko & López-Sepulcre, 2007; Bascompte & Jordano, 2007; Guimarães *et al.*, 2011; Nuis-
75 mer *et al.*, 2012). However, demography may influence trait evolution (Pelletier *et al.*, 2007). Yet,
76 eco-evolutionary spatial dynamics models combining simultaneously population and trait dynamics
77 to connect trait-based patterns as complementarity and convergence with nestedness in mutualistic
78 networks are currently lacking.

79 Recently, Guimarães *et al.* (2011) and Nuismer *et al.* (2012) explored evolutionary models using a
80 broad range of coevolutionary selection values to study convergence and complementarity in mutu-
81 alistic networks. Guimarães *et al.* (2011) show that convergence in a one-dimensional trait within a
82 trophic level may in part emerge as a consequence of selection for a complementarity trait between
83 trophic levels. For weak or absent coevolutionary selection, Nuismer *et al.* (2012) show that trait val-
84 ues in animal and plant species can be highly variable and non-convergent but positively correlated
85 (i.e., complementary). As coevolutionary selection intensifies, variation in the trait values of animal
86 and plant species is reduced and convergence emerges but correlations between traits of interacting
87 species are weakened (i.e., low pairwise complementarity). Nuismer *et al.* (2012) further explored
88 the connection between convergence and complementarity to nestedness patterns in mutualistic net-
89 works. They showed that interactions mediated by a mechanism of phenotype matching tend to be
90 antinested when coevolutionary selection is weak and become even more strongly antinested with in-
91 creasing coevolutionary selection favoring the emergence of reciprocal specialization. Taken together,
92 these results suggest that it is not trivial to explain simultaneously a high degree of convergence,
93 complementarity and nestedness in species-rich mutualistic networks as observed the empirical data.

94 Difficulties in obtaining predictions of simultaneously large values of convergence, complementarity
95 and nestedness in mutualistic networks may also be a consequence of unexplored drivers currently
96 lacking in models of mutualistic networks. Such unexplored drivers can be models of diversifica-
97 tion dynamics. Much work on diversification emphasizes on ecological divergence and speciation
98 (Schluter, 2009; Doebeli, 2011; Seehausen *et al.*, 2014; Rainey & Travisano, 1998; Butlin *et al.*, 2009;
99 Gavrillets & Losos, 2009), but we propose here to step back and ask basic questions about the dy-
100 namics of divergence in mutualistic networks, and how it depends on sexual reproduction, spatial,
101 genetic, morphological and demographic processes. Before we understand the full impact of adap-
102 tation and coevolutionary selection on evolution and diversity in ecologically complex mutualistic
103 networks, we need to understand well the basic dynamics of mutation, gene flow, drift, morpholog-
104 ical and spatial constraints underlying the process of diversification. Thus, to further understand
105 the trade-offs between convergence, complementarity and nestedness in mutualistic networks, di-
106 versification models accounting for phylogenetic relatedness combining demographic, morphological
107 constraints and evolutionary processes of trait divergence and convergence in species-rich mutualis-

108 tic networks are required. Diversification models can connect landscape genetics with community
109 dynamics (Gavrilets *et al.*, 2000; de Aguiar *et al.*, 2009; Melián *et al.*, 2012; Higgs & Derrida, 1992)
110 and combine main evolutionary forces (mutation, recombination, genetic drift, speciation and ex-
111 tinction) with demographic processes (migration and ecological drift) (Kimura, 1983; Hubbell, 2001;
112 Lynch, 2007b; Vellend, 2010)). Therefore, they may provide a benchmark to distinguish neutral from
113 niche-based or coevolutionary selection processes in predicting the connections between convergence,
114 complementarity and nestedness in empirical mutualistic networks. Here, we extend landscape genet-
115 ics models of diversification dynamics to connect quantitative trait dynamics in sexually reproducing
116 plant and pollinator populations to convergence, complementarity and nesstedness in mutualistic
117 networks.

118 We find that diversification dynamics significantly change trait distributions, and patterns of con-
119 vergence, complementarity, nestedness and connectance in mutualistic networks. We show that
120 convergence and complementarity emerge together with high levels of nestedness in the absence of
121 coevolutionary selection. Trait convergence occurs mostly between the common species and on aver-
122 age in approximately $17.3 \pm 6\%$ of all possible events while trait complementarity occurs in $20 \pm 18\%$
123 of all possible events. Qualitative comparison with empirical data show that these values are lower
124 than the high levels of convergence and complementarity observed in empirical networks (Bascompte
125 & Jordano, 2007). In contrast to previous studies where interactions mediated by a mechanism of
126 phenotype matching tended to be antinested when coevolutionary selection was weak, we found that,
127 in the absence of coevolutionary selection, highly nested values are obtained in agreement with the
128 empirical mutualistic networks. Taken together our results suggest that diversification dynamics
129 combining ecological (demography and dispersal limitation), population genetics (mutation, recom-
130 bination, assortative mating and drift) and morphological constraints associated to trait matching
131 expand theoretical approaches to predict the key patterns of mutualistic networks, from trait con-
132 vergence and complementarity to connectance and nestedness.

133 The model: Eco-evolutionary diversification in mutualistic networks

134 We consider a landscape consisting of several individual plants (P) and animal pollinators (A).
135 Individuals belonging to these two communities interact mutualistically and we assume obligate
136 mutualism for both partners. Furthermore, we assume that the number of individuals at each trophic
137 level is fixed and equal to the environmental carrying capacity for the given community. Genetic,
138 phenotypic and species composition change in time and space due to replacement of dead individuals
139 by offspring of the same or another species (the key terms and model steps are summarized in figure
140 1 and table 1, respectively). In this section we explain how we model population, diversification and
141 trait dynamics.

142 Population dynamics

143 Our model is a stochastic individual-based model with overlapping generations. The population
144 consists of J_P and J_A haploid gonochoric (i.e. separated sexes) individuals with an explicit genome
145 of size L each and equal sex ratios at the outset. The genome of each individual is composed of set
146 of $L - 1$ assortative mating loci and one neutral locus. Both plant and animal population reproduce
147 sexually and are spatially structured. At each time step an individual plant k and animal k' are
148 randomly selected to die. There are four conditions for producing viable offspring for the plant and
149 animals, concerning: 1) geography, 2) genetics, 3) obligate mutualism and 4) morphology:

150 1. Geography: a female and a male individual within the plant and animal populations are ran-
151 domly chosen among all females and males within a distance d_{max} of the dead plant k and dead
152 animal k' . This requires two geographic distance matrices, one for plants, $D^P = [d_{ij}^P]$, and one
153 for animals, $D^A = [d_{ij}^A]$, containing all the pairwise distances.

154 2. Genetics: to produce a viable offspring between the female and the male in the plant and
155 animal populations, they must have a genetic similarity value of the assortative mating loci,
156 $q_{\varnothing\sigma}$, higher than the minimum genetic similarity to have viable offspring, q_{min} , ($q_{\varnothing\sigma} > q_{min}$).
157 This process reflects assortative mating and it requires two genetic similarity matrices, one for
158 plants, $Q^P = [q_{ij}^P]$, and one for animals, $Q^A = [q_{ij}^A]$, containing all the pairwise similarity values.

- 159 3. Obligate mutualism: that the geographic distance between the female ♀ (animal or plant)
 160 and one of the two male animal or plant individuals, represented here as j , is lower than the
 161 maximum distance, d_{max}^{PA} , ($d_{j\text{♀}}^{PA} < d_{max}^{PA}$). This requires one geographic distance matrix, $D^{PA} =$
 162 $[d_{ij}^{PA}]$, containing all the pairwise distances.
- 163 4. Morphology: female plants need the presence of an animal pollinator with a larger or equally-
 164 sized proboscis than the corolla of the female plant, thus the phenotype of the selected polli-
 165 nator, represented here as j , must satisfy $z_{\text{♀}}^P \leq z_j^A$. This requires two phenotype distributions,
 166 one for the plants, $Z^P = [z_i^P]$ and one for the animals, $Z^A = [z_i^A]$. This mechanism is similar
 167 to the the “phenotypic difference” mechanism assumed in the model of Nuismer *et al.* (2012).

168 The offspring arising from this mating event will occupy the geographic position of the just deceased
 169 individual.

170 Neutral locus evolution

171 We considered a neutral locus to estimate the genetic differences or divergence among species for the
 172 calculation of convergent events (see Section Evolutionary convergence). This neutral locus is located
 173 at the end of the genome at the position L and has k possible allelic states. The locus is assumed to
 174 be completely unlinked from the rest of the genome (i.e. the assortative mating loci). We assumed
 175 a specific low mutation rate of $\mu_{neutral} = 10^{-7}$ and the k allele mutation model (i.e. model in which
 176 each allele can mutate to any of the other $k-1$ possible alleles with equal probability) (Hoban et al,
 177 2013). To calculate the genetic differences among species of the we used the Cavalli-Sforza distance
 178 (Cavalli-Sforza & Edwards, 1967) and constructed a matrix of genetic distances among species.

179 Diversification dynamics

180 To quantify speciation events we calculate the genetic distance between each pair of individuals based
 181 on the assortative mating loci. We represent the genome of each individual by a sequence of $L - 1$
 182 loci, where each locus can be in two allelic states, $+1$ or -1 . The assortative mating loci of each
 183 plant individual i in a population of size J_P is represented as a vector: $S^i = (S_1^i, S_2^i, \dots, S_L^i)$, where
 184 S_u^i is the u^{th} locus of individual i . The genetic similarity based on assortatove mating loci between

185 individuals i and j is calculated as the sum of identical loci across the genome

$$q_{ij}^P = \frac{1}{L} \sum_{u=1}^L S_u^i S_u^j \quad (1)$$

186 where $q_{ij}^P \in \{-1, 1\}$ with the genetic similarity matrix, $Q^P = [q_{ij}^P]$, containing all pairwise genetic
187 similarity values for plants (the same for animals, $Q^A = [q_{ij}^A]$). The genome of the offspring is obtained
188 by a block cross-over recombination of a female genome, S^{φ} , and a male genome, S^{σ} , where a locus
189 l in the genome of the parents is randomly chosen partitioning the genome of each individual in
190 two blocks. All genes beyond that locus l in either genome are swapped between the two parents
191 and eventually form two new genomes. One of the two new genomes is randomly chosen for the
192 offspring. The offspring's genome undergoes mutations at mutation rate μ . Figure 1 describes the
193 recombination-mutation process.

194 At the beginning of the simulations all individuals are genetically identical (all q_{ij}^P and $q_{ij}^A =$
195 1); hence they are all able to mate and produce viable offspring. The genetic similarity between
196 individuals of a guild can be visualized as an evolutionary spatial graph (Melián *et al.*, 2010), where
197 nodes correspond to individuals and the edges correspond to the geographic distances between a pair
198 of individuals satisfying the genetic similarity condition for mating, $q_{ij}^P(q_{ij}^A) > q_{min}$. The connectance
199 of the graph will decrease when generations move forward because of the processes described in
200 the previous section: 1) spatial constraints for mating driving assortative mating and dispersal
201 limitation; 2) genetic divergence driven by the threshold for mating (incompatibilities), mutation
202 and recombination forming the genome of the offspring; 3) obligate mutualistic interactions driven
203 by spatial proximity of individuals of the other guild, and 4) morphological constraints.

204 These four set of processes drive genetic divergence and speciation. We followed the species defi-
205 nition of Nei *et al.* (1983), which states that species are groups of individuals that are reproductively
206 isolated and can interbreed to produce fertile offspring. In our model this is realized through al-
207 lowing two individuals to mate successfully if their genetic similarity value is larger or equal to the
208 minimum value, q_{min} . Thus, speciation is defined as a group of genetically related individuals, where
209 two individuals in a sexual population can be conspecific while also being incompatible, as long as
210 they can exchange genes indirectly through other conspecifics (de Aguiar *et al.*, 2009; Melián *et al.*,
211 2010). This is the definition of 'ring species' (Moritz & Schneider, 1992).

Genetic divergence will eventually produce the formation of two genetically incompatible clusters of individuals, i.e. two species. This speciation process, also called 'fission-induced' speciation, continues to form more clusters and genetic divergence between individuals of different species increases. However, the diversification dynamics will fluctuate due to random extinctions (death of last individual of a species). A stochastic balance between speciation and extinction is eventually reached giving the final steady-state of the metacommunity.

Quantitative trait dynamics

We model each individual plant and animal with a quantitative trait, z^P and z^A , respectively. The processes described in figure 1 govern two quantitative traits, one for each guild: proboscis or bill length (z_i^A) in pollinators and corolla length (z_i^P) in plants. The quantitative trait of offspring is determined by the additive genetic effects of the genome (i.e. no epistasis) after the process of randomly choosing one of the new two genomes and mutation (figure 1) plus a normally distributed environmental effect, ϵ , $\mathcal{N}(\mu_\epsilon = 0, \sigma_\epsilon^2 = 1)$ (Guimarães *et al.*, 2011). The phenotype of the plant offspring i is $z_i^P = g_i^P + \epsilon$ and the genetic component (g_i^P) of the phenotype of offspring i is

$$g_i^P = L + S_o^i \quad (2)$$

with $S_o^i = \sum_{u=1}^L S_u^i$. Hence g_i^P is calculated as the sum of alleles across the genome (Kondrashov & Shpak, 1998) plus the number of loci to avoid negative trait values (g_i^A is calculated similarly for animals). We assumed that the magnitude of the influence (i.e., effect sizes) of any given locus on this quantitative trait is equal across all the loci (Seehausen *et al.*, 2014). This means that two individuals with a different combination of alleles in the genome can express the same quantitative trait (Losos, 2011).

232 Convergence, complementarity and nestedness

233 Evolutionary convergence

234 The calculation of convergence is illustrated in figure 2 (To visualize the genetic relatedness between
235 species we constructed clustering trees using Euclidean distance with the Python library ETE 2.01
236 (Huerta-Cepas *et al.*, 2010)). It requires computing pairwise genotypic and phenotypic similarities
237 and the similarity between mean species phenotypes from distantly related species. With only three
238 species, only one convergence is possible after excluding the sister species. The number of conver-
239 gences potentially increases with the number of species present. For example, if we have ten species
240 and we exclude one of them as the sister species of the focal species, we have nine species to cal-
241 culate convergence for. If we find that two out of nine species are phenotypically similar enough
242 to the focal species, we count two (out of nine, $\sim 22\%$) convergences. We repeat this by changing
243 the focal species and calculate the mean convergence events over all species. In contrast to previ-
244 ous approaches that used the mean pair-wise difference between traits of species (Guimarães *et al.*,
245 2011) or the variance of species traits in a guild as a proxy to predict convergence (i.e., large values
246 weak convergence whereas small values of the variance may indicate strong convergence, (Nuismer
247 *et al.*, 2012)), we used the relationship between genetic divergence and phylogenetic relatedness for
248 the estimation of evolutionary convergences. The advantage of our method considering phylogenetic
249 relatedness is that it excludes cases of development of very similar trait values from sister species
250 (i.e., parallel evolution, (Losos, 2011)) and therefore it does not overestimate convergence events.

251 Phenotypic similarity

252 The phenotypic similarity for plants (p_{ij}^P) between individual i and j is defined as

$$p_{ij}^P = 1 - \frac{|z_i^P - z_j^P|}{z_{max}^P} \quad (3)$$

253 where z_i^P and z_j^P are the phenotypic similarity values of i and j , respectively, and z_{max}^P is the maximum
254 value of the phenotype distribution, Z^P . Thus, the elements $p_{ij}^P \in \{0, 1\}$ of the phenotypic similarity
255 matrix, $\mathcal{P}^P = [p_{ij}^P]$ represent all pairwise values for plants (the same for animals, $\mathcal{P}^A = [p_{ij}^A]$).

256 Mean genetic and phenotypic species similarity

257 We define evolutionary convergence as the similarity between average species phenotypes from dis-
 258 tantly related species. We assume that two species are distantly related, in phylogenetic terms, if
 259 they do not come from a direct common ancestor, i.e. they are not sister species. To exclude sister
 260 species from the analysis we need to calculate the mean genetic similarity among species of the same
 261 guild. The mean genetic similarity between a plant species k and a plant species l is

$$\hat{q}_{kl}^P = \frac{1}{n_k n_l} \sum_{i=1}^{n_k} \sum_{j=i}^{n_l} q_{ij}^P \quad (4)$$

262 where q_{ij}^P is the genetic similarity between an individual i of plant species k and an individual j of
 263 plant species l , and n_k and n_l are the absolute abundances of plant species k and l , respectively. The
 264 elements \hat{q}_{kl}^P form the matrix $Q_s^P = [\hat{q}_{kl}^P]$ from which the sister species of each species in the guild can
 265 be identified (The elements for animals, $Q_s^A = [\hat{q}_{kl}^A]$, are calculated in the same way as we did for the
 266 plants). To calculate evolutionary convergence we need to know the average phenotypic similarity
 267 between two species. We define phenotypic similarity between species k and l as

$$\hat{p}_{kl}^P = \frac{1}{n_k n_l} \sum_{i=1}^{n_k} \sum_{j=i}^{n_l} p_{ij}^P \quad (5)$$

268 which is analogous to the definition of eq. 4, but now considering phenotypes instead of genotypes.
 269 This will build a species phenotypic similarity matrix $P_s^P = [\hat{p}_{kl}^P]$ (the species phenotypic similarity
 270 matrix, $P_s^A = [\hat{p}_{kl}^A]$, is calculated analogously for the animals). We then focus on each species in
 271 turn and exclude its sister species to avoid cases of parallel evolution to calculate the number of
 272 convergences related to the focal species. We define a focal plant species k and a non-sister plant
 273 species l to be convergent if phenotypic similarity between them is higher than between focal and
 274 sister species ($\hat{p}_{k,sister}^P < \hat{p}_{kl}^P$) and higher than a certain phenotypic threshold value h_{conv} ($\hat{p}_{kl}^P > h_{conv}$);
 275 convergent species is calculated analogously for the animals).

276 Evolutionary complementarity

277 Evolutionary complementarity does not require the genetic similarity matrix. We only need to
 278 estimate the phenotypic similarity between plant and animal species and we do this as we did for the

279 evolutionary convergence. We calculate the phenotypic similarity matrix $P_s^{PA} = [\hat{p}_{kh}^{PA}]$. This matrix
 280 contains the mean trait similarity for each plant species k and animal species h . The condition
 281 for complementarity is that the similarity between a plant species k and an animal species h is
 282 $\hat{p}_{kh}^{PA} > h_{compl}$, where h_{compl} is the phenotypic threshold value to detect a complementarity event.

283 Plant-animal interactions

284 In addition to the genetic and geographic constraints for mating, we consider two other conditions for
 285 plants and animals: obligate mutualism and morphological constraints. Obligate mutualism applies
 286 to the plants and animals to reproduce but the morphological constraints only apply to plants. We
 287 therefore need a geographic distance matrix, D^{PA} , to describe the geographic distance between plant
 288 and animal individuals. Plant-animal mutualistic interactions are here described as follows: plants
 289 benefit from the presence of specific pollinators that are able to pollinate them and animals benefit
 290 from the presence of plants that provide resources for them. Thus, we have two extra conditions for
 291 mating:

- 292 1. Female plants need the presence of an animal pollinator (i.e., male and female represented as
 293 j) within a close distance, $d_{j\Phi}^{PA} < d_{max}^{PA}$. The pollinator must have a larger or equally-sized
 294 proboscis than the corolla of a plant, $z_{\Phi}^P \leq z_j^A$. This corresponds to a morphological constraint
 295 for individual interactions observed between plant and pollinator species (Stang *et al.*, 2009,
 296 2006).
- 297 2. Animals need the presence of a plant (male or female represented as j) within a close geographic
 298 distance, $d_{jk}^{PA} < d_{max}^{PA}$.

299 Our model allows bookkeeping of who is interacting with whom, i.e. this means we can record ex-
 300 actly which plant and animal individuals are interacting. This bookkeeping enables us to identify the
 301 consequences of geography, genetics, obligate mutualism and morphology for the evolution and final
 302 topology of the network. We record the identity of the mutualistic partners during the reproduc-
 303 tion process for plants and animals after reaching the steady-state to reconstruct the plant-animal
 304 interaction network.

305 Nestedness and connectance

306 To study the connection between convergence and complementarity with network properties, we mea-
307 sured two topological properties of plant-animal mutualistic networks: nestedness and connectance.
308 We estimated nestedness using the NODF algorithm developed by (Almeida-Neto *et al.*, 2008) be-
309 cause of its statistical robustness. NODF is based on standardized differences in row and column fills
310 and paired matching of occurrences. Connectance measures the proportion of realized interactions
311 among all possible interactions in a network. It is defined as $C = \frac{k}{P \times A}$, where k represents the number
312 of realized interactions between plant and animal species and P and A represent the number of plant
313 and animal species in the network, respectively (Jordano *et al.*, 2003).

314 Simulations

315 We simulated equal population sizes for plants and animals with $J^P = J^A = 1,000$ individuals.
316 Genome size, L , of each individual was 150 loci. Initial trait distributions for the plants, $Z^P = [z_i^P]$
317 and animals, $Z^A = [z_i^A]$, were generated following equation 2 plus a normally distributed environ-
318 mental effect, ϵ , $\mathcal{N}(\mu_\epsilon = 0, \sigma_\epsilon^2 = 1)$. To ensure plant mating conditions are met at the beginning of
319 the simulation all animal individuals have a higher phenotypic trait value than the plant individuals.

320 Geographic distances between each pair of individuals i and j for the plants, d_{ij}^P , and animals,
321 d_{ij}^A , were calculated as follows: 1) Euclidean coordinates of a two-dimensional space (x_i, y_i) were
322 sampled from a uniform distribution $(x_i = [0, 1], y_i = [0, 1])$ for each individual for the plants and
323 animals; 2) Using these coordinates we calculated a matrix of relative Euclidean distances between
324 the individuals for the plants, d_{ij}^P , and animals, d_{ij}^A . This set-up is similar to that of Melián *et al.*
325 (2010). This procedure was repeated for each of the geographic distance matrices (D^{PA}, D^P, D^A) .

326 We ran 2,000 generations for each replicate for a total of 500 replicates, where a generation is
327 the update of the effective population size ($J^P = J^A = 1,000$), i.e. the number of steps equal
328 to the effective population size. Steady-state was verified by checking the constancy of speciation
329 events during the last 100 generations. We calculated convergence, complementarity, nestedness and
330 connectance at steady-state. Convergence and complementarity events were calculated for a whole
331 range $([0.0, 1.0])$ of their respective thresholds, h_{conv} and h_{compl} . We explored parameter combinations

with mutation rate, $\mu \in \{10^{-4}, 10^{-2}\}$, minimum genetic similarity, $q_{min} = 0.97$, maximum distance for finding a mate and disperse, $d_{max} \in \{0.1, 0.3\}$, and a maximum geographic distance to find a mutualistic partner, $d_{max}^{PA} = 0.3$. We implemented the model in Python (and tested in IPython (Pérez & Granger, 2007)). Plots were produced using the Python library Matplotlib (Hunter, 2007).

Model-data fitting

We test our model's predictions of convergence and complementarity using a morphological dataset of a plant-hummingbird community from Maglianesi *et al.* (2014). More specifically, we used the data about corolla length and bill length from plants and hummingbirds, respectively. To calculate convergence with this empirical dataset we also considered the phylogenetic relationships among species. We used a well resolved phylogeny of hummingbirds by McGuire *et al.* (2007), from which we could only used XX hummingbird species from a total of YY, which were not present at the phylogenetic tree. However, for the plant species we had to construct a phylogenetic tree using genetic data of XXXX taken from genBANK and calculate a ML tree using RAXML . We excluded XX species from the analysis (see Suppl. Materials) because their phylogenetic relationships were not well resolved (polytomies), leaving a total of ZZ species from a total of YY from the dataset of Maglianesi et al (2014). We used the R package APE (Paradis *et al.*, 2004) in R (R Core Team, 2013) to visualize and prune the tips (species) that were not used in our analysis (see Suppl. Materials)

We used the phylogenetic trees with their respective branch lengths to calculate a genetic distance matrix among species. Using both phylogenetic trees (hummingbirds and plants) we simulated nucleotide sequences of 100bp with the program SeqGen (Rambaut & Grassly, 1997) assuming the Juke-Cantor model of molecular evolution. These simulated sequences were then used to calculate the genetic distance matrix using the R package *seqinr* in R (R Core Team, 2013) and finally obtain the genetic similarity matrix. Finally, to calculate the convergence values of the empirical data, we generated 1000 replicates from the simulations (bootstrapping) and each replicate contained the same number of plant and animal species as the empirical data. Complementarity and convergence were calculated for each of the replicates. Complementarity and convergence were calculated as explained above . However, we also calculated convergence events assuming a more conservative

estimation where we excluded 30 % of species that were genetically similar to the focal species,
instead of only the sister species.

Results

Population dynamics and diversification dynamics changed plant and animal community trait distributions (i.e. corolla and proboscis lengths) with bimodal distributions being the most commonly produced patterns across replicates (figure 3). At species level, a gradient of species phenotypes with common species presenting lower mean and higher variance than rare species emerged. Mean and variance of the trait values were correlated for most replicates (Spearman- $\rho > 0.41$, $p < 0.05$) and the distributions of abundance for plant or animal species were highly skewed and significantly different from a normal distribution (Lilliefors's test, all $p < 0.001$). Abundance predicted plant or animal mean species traits in approximately 70% of the replicates (Spearman- $\rho > 0.32$, $p < 0.05$) and trait variance for all replicates ($0.39 < \text{Spearman-}\rho < 0.79$, all $p < 0.05$). Mean and variance of species trait values significantly differed between common and rare plant or animal species (inset in figure 3) suggesting a strong impact of diversification by producing a gradient of species phenotypes in mutualistic networks.

Evolutionary convergence events occurred in all replicate simulations (see equations 4 and 5 with an example of evolutionary convergence events in animals and plants represented in figure 4). Convergence events were heterogeneously distributed across species with most events occurring between common species ($0.42 < \text{Spearman-}\rho < 0.89$, all $p < 0.05$). Evolutionary convergence occurred on average in $17.3 \pm 6\%$ of all possible convergence events with more than 95% of these events occurring within the three most common species. These results show that evolutionary convergence is not randomly distributed across pairs of species but highly aggregated during the diversification process. Evolutionary convergence can also be visualized using a scatter plot of the genotype-phenotype map for all pairs of individuals within the plant and animal communities (figure 5). As expected from equation 2, there is a positive genotype-phenotype relationship. The scatter plot contains three main clouds of points that consistently occur in our simulations for the plants, P , and animals, A : 1) pairs of individuals of the same species with high genetic ($q_{ij} > q_{min}$) and phenotypic ($p_{ij} > 0.9$) similar-

ity, 2) pairs of individuals of the same species with genetic similarity below q_{min} ($q_{ij} < q_{min} = 0.97$) and high phenotypic similarity ($p_{ij} > 0.9$). These are incompatible individuals for mating, yet with high phenotypic similarity, $p_{ij} > 0.9$, and 3) highly genetically dissimilar individuals from different species, $q_{ij} \ll q_{min}$, but with the presence of highly phenotypically similar individuals ($p_{ij} > 0.9$). This last category shows evidence of evolutionary convergence between species in plants and animals. An increase in mutation rate increases the genetic divergence between species, as expected, but it does not change the genotype-phenotype relationship qualitatively (see figure 5).

Evolutionary complementarity occurred with a similar frequency as evolutionary convergence in each replicate (see equation 5 and compare the initial with the final trait distributions in figure 3), but with a larger variation ($20 \pm 18\%$). Connectance values were consistently medium or high ($\bar{C} = 0.5 \pm 0.07$, figure 6), mostly larger than reported in empirical data (table 2). Nestedness values were always high ($\bar{N} = 69.97 \pm 13.4$ (figure 6)), as in empirical plant-pollinator networks (table 2).

Convergence, complementarity and nestedness did not show signs of trade-offs and were uncorrelated across all replicates ($0.08 < \text{Spearman-}\rho < 0.27$, all $p > 0.1$) with the exception of a positive correlation between trait complementarity and evolutionary convergence in the plant community (Spearman- $\rho = 0.61$, all $p < 0.05$). These results suggest a low to medium convergence and complementarity regardless of the initial parameter combination explored and these values are qualitatively lower than the values reported in the literature for empirical mutualistic networks (see table 2). In summary, using phylogenetically relatedness and phenotypic similarity for the estimation of evolutionary convergence and complementarity in the absence of coevolutionary selection, our results show evolutionary trait convergence and complementarity in all our replicate simulations but with little and large variation, respectively. For weak or absent coevolutionary selection, trait convergence in plant and animal communities is largely independent or positively correlated with trait complementarity for the animal and plant community, respectively. These results show that high levels of convergence, complementarity and nestedness are never reached together. However, our results show that it is possible to reach consistently low to medium convergence and complementarity together with high levels of nestedness in the absence of coevolutionary selection and convergence-complementarity trade-offs.

Convergence predictions with empirical data

We found that our predictions of convergence events were very close to observed convergence values of the hummingbird community for all the range of threshold values (see Figure X.a). However, the predicted values of convergence for the plants were higher than the observed values of the plant community across all the range of threshold values (see Figure X.b).

Discussion

We have extended previous landscape genetics models (de Aguiar *et al.*, 2009; Melián *et al.*, 2012) to connect population and diversification dynamics with quantitative trait dynamics to study trait complementarity, convergence and nestedness in species-rich mutualistic networks. Our results show high levels of nestedness combined with low to medium levels of convergence and complementarity after controlling for phylogenetic relatedness. This partly deviates from the simultaneously high levels of nestedness, convergence and complementarity (Guimarães *et al.*, 2011; Nuismer *et al.*, 2012) observed in empirical data (Bascompte & Jordano, 2007). After controlling for phylogenetic relatedness and phenotypic similarity, we show that evolutionary trait convergence is observed in all our replicate simulations with little variation ($17.3 \pm 6\%$) and it is heterogeneously distributed across species with most events occurring between the common species. This suggests that evolutionary convergence is not randomly originated across pairs of species but highly aggregated during the diversification process. Complementarity is consistently observed but with a larger variation than convergence $20 \pm 18\%$. In summary, our analysis suggests that convergence, complementarity and nestedness do not show signs of trade-offs in the absence of coevolutionary selection. In fact, we even obtained a positive trait complementarity and evolutionary convergence correlation in the plant community. This suggests that the basic genetic and ecological processes considered here can produce this positive correlation between complementarity and convergence.

Previous studies have argued that evolutionary convergence is the product of multispecific coevolutionary processes ('diffuse coevolution')(Janzen, 1980; Thompson & Cunningham, 2002; Jordano *et al.*, 2003; Bascompte & Jordano, 2007) and therefore convergence events are molded by similar ecological (or niche) selective pressures. Recent mutualistic coevolutionary models assuming the

mechanism of 'phenotypic difference' (as our model) have shown that for weak or absent coevolutionary selection trait values in animal and plant species can be highly variable and non-convergent, but trait values of animal and plants species show high complementarity (i.e. they are positively correlated) (Nuismer *et al.*, 2012). As coevolutionary selection intensifies, variation in the trait values of animal and plant species is reduced and convergence increases, but correlations between traits of interacting species are weakened (i.e., low pairwise complementarity). However, Guimarães *et al.* (2011) have shown that trait convergence may in part emerge as a consequence of selection for a complementarity trait between the plants and animals. These approaches used all the species (Guimarães *et al.*, 2011) or the variance as a proxy to predict convergence (i.e., large values weak convergence whereas small values of the variance may indicate strong convergence, (Nuismer *et al.*, 2012)) and they might overestimate convergence events because they do not consider phylogenetic relatedness. Using phylogenetic relatedness and phenotypic similarity for the estimation of evolutionary convergences in the absence of coevolutionary selection, we show that evolutionary trait convergence and complementarity is observed in all our replicate simulations but with little and large variation, respectively. Our results contrasts with previous findings (Nuismer *et al.*, 2012) that under weak or absent coevolutionary selection we always find convergence and these convergence values are largely independent of the degree of trait complementarity between plant and animals for the animals, but positively correlated between plant and animals for the plant community.

Interestingly, the mechanism of plant-animal interaction considered in our model, where the trait of the animal needs to be equal or larger than the trait of plant ('phenotypic difference'), has shown to make unlikely the evolution of convergence and complementarity by coevolutionary selection (Nuismer *et al.*, 2012). However, our model shows that considering non-selective processes it is possible to observe the evolution of both convergence and complementarity, although in low levels compared to observed trait patterns in mutualistic webs (Bascompte & Jordano, 2007). It remains to be seen whether the action of both (selective and non-selective forces) will be able to generate the observed patterns of high convergence and complementarity.

Non-selective forces can produce convergence. For example, Stayton (2008) simulated evolution along phylogenies according to a Brownian motion model of trait change and demonstrated that rates of convergence can be quite high when clades are diversifying under only the influence of genetic drift.

470 Furthermore, other type of constraints in the production of variation can also lead to convergence.
471 If the variation produced is limited, then unrelated species are likely to produce the same variation,
472 which may then become fixed in the population by genetic drift (Stayton, 2008; Losos, 2011). This
473 may be common feature of biological systems because DNA contains only four possible states for a
474 given nucleotide position, and therefore it is likely that distantly related taxa will independently ac-
475 quire the same change by chance regardless of the environmental conditions or niche-driven dynamics
476 (Losos, 2011). Developmental constraints or the evolution of genetic networks by non-adaptive pro-
477 cesses may also be explanations for the convergence of traits (Solé *et al.*, 2002; Lynch, 2007a; Losos,
478 2011), but the role of developmental constraints or genetic networks in determining convergence in
479 species-rich mutualistic networks has yet not been explored. For example, the tinkering of traits
480 by evolutionary forces largely affects developmental pathways (e.g. gene regulatory networks) (Solé
481 *et al.*, 2002). Developmental pathways are not static but can diverge through time randomly without
482 substantially affecting the phenotype (Wagner, 2008). This concept, also called developmental sys-
483 tem drift (DSD) (True & Haag, 2001), might play an important role in the evolution of convergence
484 in morphological traits and it should be considered as another process where drift can act (Ohta,
485 2002), for example, by random wiring in gene regulatory networks. Our results based on a method
486 that excludes cases of the development of a similar trait in related but distinct species descending
487 from the same ancestor (i.e., parallel evolution, (Losos, 2011)) show that additional constraints such
488 as dispersal limitation, obligate mutualisms and assortative mating limit the production of variation
489 and lead consistently to convergence in species-rich mutualistic networks.

490 Evolutionary complementarity is also consistently observed in our results but with a larger variation
491 than convergence. Complementarity is argued to be the main result of tight coevolution between
492 mutualistic species by mechanisms, such as trait-matching (e.g. corolla length-proboscis length)
493 (Jordano *et al.*, 2003). There is empirical (Anderson & Johnson, 2008) and theoretical evidence
494 (Gomulkiewicz *et al.*, 2000) for coevolutionary hot spots (Thompson, 1999), which suggests that
495 local selective regimes can promote the coevolution of traits (Gomulkiewicz *et al.*, 2000; Ferdy *et al.*,
496 2002; Gomulkiewicz *et al.*, 2003; Jordano *et al.*, 2003; Bronstein *et al.*, 2006; Thompson & Cunning-
497 ham, 2002; Thompson, 2009; Jones *et al.*, 2009). Our results show that low to medium levels of
498 complementarity can emerge from relatively non-selective forces and constraints occurring at several

499 levels, from geographic limits to encounter partners and disperse to the genetic and morphological
500 constraints on producing viable offspring.

501 Our model predicts that the distribution of traits, regardless of species differences, generally evolves
502 towards a bimodal distribution of phenotypes. This result was previously obtained by Kondrashov &
503 Shpak (1998), who assumed absence of selection and assortative mating in a infinite population. Their
504 result with strong assortative mating produces high correlations of allelic effects among all loci, which
505 leads to the evolution of two phenotypic classes: one with alleles increasing the trait and the other
506 with alleles decreasing the trait (Crow & Kimura, 1970). Devaux & Lande (2008) found similar results
507 using a finite diploid population with multiple alleles per locus and they showed that the splitting
508 of the phenotype distribution is possible under strong assortative mating and genetic drift, but the
509 distribution is transient rather than permanent. In our model the distribution is not transient, and
510 this may be probably due to having only considered two allelic states, instead of multiple allelic
511 states, for each locus. As Devaux & Lande (2008) explained, by assuming a normal distribution of
512 allelic effects at each locus we could obtain a more continuous unimodal (i.e. normal) distribution
513 of phenotypes. We need further analytical exploration to thoroughly understand the determinants
514 of trait distributions in our model. Nevertheless, we find a gradient of species phenotypes from low
515 to high mean trait values (Insets in figure 3), but trait distributions for the parameter combination
516 explored are not right-skewed, as observed in real plant-pollinator communities (Stang *et al.*, 2009)
517 (see Table 2). This might be due to the influence of other traits not considered in our model, such
518 as forbidden links (e.g. body size) and developmental constraints.

519 Nuismer *et al.* (2012) explored the connection between convergence and complementarity to nest-
520 edness patterns in mutualistic networks. They show that coevolutionary selection tend to decrease
521 nestedness and it generates even more strongly antinested networks when coevolutionary selection
522 increases by favoring the emergence of reciprocal specialization. In contrast, nestedness values were
523 very high in our model, as in real mutualistic networks. Previous neutral models taking into account
524 ecological drift (Krishna *et al.*, 2008; Canard *et al.*, 2012), produced high values of nestedness which
525 suggests that random interactions and species abundance distribution ('neutral forbidden links' (Ca-
526 nard *et al.*, 2012)), are determinants of the structure of mutualistic networks. Connectance values
527 obtained from our simulations are close to the predictions of other neutral network models (Canard

528 *et al.*, 2012). However, compared to real mutualistic networks with similar diversity as ours (24
529 plant and animal species on average), our connectance values ($\bar{C} = 0.5$) are higher than the reported
530 webs ($C = 0.28$) (Olesen & Jordano, 2002). Interestingly, Nuismer *et al.* (2012) found that only
531 assuming coevolutionary selection forces also leads to an increase in connectance. This means that
532 both basic genetic and ecological processes and coevolutionary selection can increase connectance in
533 mutualistic networks. The question is why observed mutualistic webs have a lower connectance than
534 those predicted by our model and those considering coevolutionary selection? We conjecture that
535 this difference in connectance values might be due to different types of forbidden links (i.e. biological
536 constraints impeding plant-animal interactions), such as phenology (Encinas-Viso *et al.*, 2012; Olesen
537 *et al.*, 2008), body size (Olesen *et al.*, 2010) or environmental fluctuations that were not explicitly
538 included in our approach.

539 High values of the required genetic similarity to produce viable offspring, q_{min} , and shorter geo-
540 graphical distances for mating (d_{max}) lead to higher species diversity in models with one metacom-
541 munity (Melián *et al.*, 2012), but low geographic distances for mating could decrease species diversity
542 due to the difficulty of finding mates (i.e., Allee effect) or due to inbreeding, especially for high genetic
543 similarity threshold values to produce viable offspring. In our model we assume that genetic incom-
544 patibilities, assortative mating and morphological traits are determined by the same multiple loci
545 (i.e. they have the same genetic basis) and these genes show pleiotropic effects. We do not explicitly
546 model how incompatibilities accumulate (Welch, 2004) and assortative mating and morphological
547 traits are calculated in a similar way: we sum genetic differences regardless of the magnitude of the
548 influence (i.e., effect sizes) of any given locus on this quantitative trait (Seehausen *et al.*, 2014). This
549 means that two individuals with different combinations of alleles in the genome can express the same
550 quantitative trait (Losos, 2011). Our interpretation of non-random mating and an ecological trait
551 may be similar to the concept of 'magic' traits (Thibert-Plante & Gavrilets, 2013). A 'magic' trait
552 combines a trait subject to divergent selection and another trait related to nonrandom mating (i.e.
553 reproductive isolation) that are pleiotropic expressions of the same gene(s) (Servedio *et al.*, 2011).
554 There are other alternatives for the relationship between assortative mating and the morphological
555 trait (Servedio *et al.*, 2011). For instance, assortative mating and the morphological trait may be
556 determined by different sets of genes and express different levels of pleiotropic effects (i.e. a partial

557 'magic' trait (van Doorn & Weissing, 2001)). One might also explore further the influence of the
558 morphological constraint on the evolution of traits. In our model, this constraint might be exerting
559 weak selection on the plant traits because some pollinator individuals may be able to interact with
560 a larger number of plants. The comparison with other models without any morphological constraint
561 (i.e. only non-random mating) and with morphological constraints for animals and plant reproduc-
562 tion (i.e. phenotypic matching) might elucidate the importance of morphological constraints in the
563 evolution of mutualistic networks.

564 In summary, our results show that the emergence of convergence, complementarity and network
565 structure is possible assuming basic genetic and ecological processes. However, we did not find high
566 levels of convergence and complementarity as observed in empirical webs, which suggests that the
567 joint action of non-selective and selective forces might generate those observed patterns. The emer-
568 gence of certain network structure properties similar to those observed in empirical webs is observed
569 in our model. In contrast to previous studies that found antinested networks when considering co-
570 evolutionary selection, we found that, in the absence of coevolutionary selection, highly nested values
571 are obtained in agreement with the empirical mutualistic networks (Bascompte *et al.*, 2003). Despite
572 some deviations from empirical findings, our results suggest that diversification dynamics combin-
573 ing ecological (demography and dispersal limitation), population genetics (mutation, recombination,
574 assortative mating and drift) and morphological constraints form the basic processes producing the
575 key patterns of mutualistic networks, from trait convergence and complementarity to connectance
576 and nestedness. More generally, our model shows that it is important to consider non-selective forces
577 to explain broad evolutionary patterns and the emergence of community structure.

578 Acknowledgments

579 We thank Martina Stang and Ole Seehausen for useful discussions. FEV and RSE were supported
580 by grants from the Netherlands Organization for Scientific Research (NWO). CJM was supported by
581 the Swiss National Science Foundation (SNSF-project 31003A-144162).

582 References

- 583 de Aguiar, M., Baranger, M., Baptestini, E., Kaufman, L. & Bar-Yam, Y. (2009). Global patterns
584 of speciation and diversity. *Nature*, 460, 384–387.
- 585 Almeida-Neto, M., aes, P.G., aes, P.G., Loyola, R. & Ulrich, W. (2008). A consistent metric for
586 nestedness analysis in ecological systems: reconciling concept and measurement. *Oikos*, 117, 1227–
587 1239.
- 588 Anderson, B. & Johnson, S. (2008). The geographical mosaic of coevolution in a plant-pollinator
589 mutualism. *Evolution*, 62, 220–225.
- 590 Anderson, B., Terblanche, J.S. & Ellis, A.G. (2010). Predictable patterns of trait mismatches between
591 interacting plants and insects. *BMC Evolutionary Biology*, 10, 204.
- 592 Bascompte, J. & Jordano, P. (2007). Plant-animal mutualistic networks: The architecture of biodi-
593 versity. *Annu. Rev. Ecol. Evol. Syst.*, 38, 567–593.
- 594 Bascompte, J., Jordano, P., Melian, C.J. & Olesen, J.M. (2003). The nested assembly of plant-animal
595 mutualistic networks. *Proc. Natl. Acad. Sci. USA*, 100, 9383–9387.
- 596 Bastolla, U., Fortuna, M., Pascual-García, A., Ferrera, A., Luque, B. & Bascompte, J. (2009). The
597 architecture of mutualistic networks minimizes competition and increases biodiversity. *Nature*,
598 458, 1018–1020.
- 599 Bronstein, J.L., Alarcon, R. & Geber, M. (2006). The evolution of plant-insect mutualisms. *New*
600 *Phytol.*, 172, 412–428.
- 601 Butlin, R., Bridle, J. & Schluter, D. (2009). *Speciation and Patterns of Diversity*. Cambridge:
602 Cambridge University Press. 346 p.
- 603 Canard, E., Mouquet, N., Marescot, L., Gaston, K., Gravel, D. & Mouillot, D. (2012). Emergence
604 of structural patterns in neutral trophic networks. *Plos One*, 7, e38295.
- 605 Crow, J. & Kimura, M. (1970). *An introduction to population genetics theory*. Harper & Row
606 Publishers, New York.

- 607 Darwin, C. (1859). *On the origin of the species*. Murray.
- 608 Darwin, C. (1862). *Fertilisation of Orchids*. Murray.
- 609 Devaux, C. & Lande, R. (2008). Incipient allochronic speciation due to non-selective assortative
610 mating by flowering time, mutation and genetic drift. *Proc R Soc B*, 275, 2723–2732.
- 611 Doebeli, M. (2011). *Adaptive diversification*. Princeton University Press, Princeton, NJ.
- 612 Encinas-Viso, F., Revilla, T. & Etienne, R. (2012). Phenology drives mutualistic network structure
613 and diversity. *Ecol Lett*, 15, 198–208.
- 614 Ferdy, J., Despres, L. & Godelle, B. (2002). Evolution of mutualism between globeflowers and their
615 pollinating flies. *Journal of Theoretical Biology*, 217, 219–234.
- 616 Ferriere, R., Gauduchon, M. & Bronstein, J.L. (2007). Evolution and persistence of obligate mutual-
617 ists and exploiters: competition for partners and evolutionary immunization. *Ecology Letters*, 10,
618 115–126.
- 619 Gavrillets, S., Acton, R. & Gravner, J. (2000). Dynamics of speciation and diversification in a
620 metapopulation. *Evolution*, 54, 1493–1501.
- 621 Gavrillets, S. & Losos, J. (2009). Adaptive radiation: Contrasting theory with data. *Science*, 323,
622 732–737.
- 623 Gomulkiewicz, R., Nuismer, S.L. & Thompson, J.N. (2003). Coevolution in variable mutualisms.
624 *The American Naturalist*, 162, S80–S93.
- 625 Gomulkiewicz, R., Thompson, J.N., Holt, R.D., Nuismer, S.L. & Hochberg, M.E. (2000). Hot spots,
626 cold spots, and the geographic mosaic theory of coevolution. *The American Naturalist*, 156, 156–
627 174.
- 628 Guimarães, P., Jordano, P. & Thompson, J. (2011). Evolution and coevolution in mutualistic net-
629 works. *Ecol Lett*, 14, 877–885.
- 630 Higgs, P. & Derrida, B. (1992). Genetic distance and species formation in evolving populations. *J*
631 *Mol Evol*, 35, 454–465.

- 632 Howe, H. & Smallwood, J. (1982). Ecology of seed dispersal. *Ann Rev. Ecol. Syst.*, 13, 201–228.
- 633 Hubbell, S. (2001). *The unified neutral theory of biodiversity and biogeography*. Princeton University
634 Press, Princeton, NJ.
- 635 Huerta-Cepas, J., Dopazo, J. & Gabaldón, T. (2010). Ete: a python environment for tree exploration.
636 *BMC Bioinformatics*, 11, 24.
- 637 Hunter, J. (2007). Matplotlib: A 2d graphics environment. *Computing In Science & Engineering*, 9,
638 90–95.
- 639 Janzen, D. (1980). When is it coevolution? *Evolution*, 34, 611–612.
- 640 Jones, E., Ferrière, R. & Bronstein, J. (2009). Eco-evolutionary dynamics of mutualists and ex-
641 ploitors. *Am Nat*, 174, 780–794.
- 642 Jordano, P., Bascompte, J. & Olesen, J. (2003). Invariant properties in coevolutionary networks of
643 plant-animal interactions. *Ecol. Lett.*, 6, 69–81.
- 644 Jousset, E., Rasplus, J.Y. & Kjellberg, F. (2003). Convergence and coevolution in a mutualism:
645 evidence from a molecular phylogeny of ficus. *Evolution*, 57, 1255–1269.
- 646 Kimura, M. (1983). *The neutral theory of molecular evolution*. Cambridge University Press, Cam-
647 bridge, UK.
- 648 Kokko, H. & López-Sepulcre, A. (2007). The ecogenetic link between demography and evolution:
649 can we bridge the gap between theory and data? *Ecology Letters*, 10, 773–782.
- 650 Kondrashov, A. & Shpak, M. (1998). On the origin of species by means of assortative mating. *Proc.*
651 *R. Soc. Lond. B*, 265, 2273–2278.
- 652 Krishna, A., Guimarães, P., Jordano, P. & Bascompte, J. (2008). A neutral-niche theory of nestedness
653 in mutualistic networks. *Oikos*, 117, 1609–1618.
- 654 Law, R., Bronstein, J.L. & Ferrière, R. (2001). On mutualists and exploiters: plant-insect coevolution
655 in pollinating seed-parasite systems. *Journal of Theoretical Biology*, 212, 373–389.

- Losos, J. (2011). Convergence, adaptation, and constraint. *Evolution*, 65, 1827–1840.
- Lynch, M. (2007a). The evolution of genetic networks by non-adaptive processes. *Nature Reviews Genetics*, 8, 803–813.
- Lynch, M. (2007b). The frailty of adaptive hypotheses for the origins of organismal complexity. *Proc Natl Acad Sci USA*, 104, 8597–8604.
- Maglianesi, M., Bluthgen, N., Böhning-Gaese, K. & Schleuning, M. (2014). Morphological traits determine specialization and resource use in plant-hummingbird networks in the neotropics. *Ecology*, 95, 3325–3334.
- McGuire, J., Witt, C., Altshuler, D. & Remsen, J. (2007). Phylogenetic systematics and biogeography of hummingbirds: Bayesian and maximum likelihood analyses of partitioned data and selection of an appropriate partitioning strategy. *Syst. Biol.*, 56, 837–856.
- Melián, C.J., Alonso, D., Allesina, S., Condit, R. & Etienne, R. (2012). Does sex speed up evolutionary rate and increase biodiversity? *PloS Comput Biol*, 8, e1002414.
- Melián, C.J., Alonso, D., Vázquez, D., Regetz, J. & Allesina, S. (2010). Frequency-dependent selection predicts patterns of radiations and biodiversity. *PLoS Comput Biol*, 6, e1000892.
- Moritz, C. & Schneider, C.J. (1992). Evolutionary relationships within the ensatina es- chscholtzii complex confirm the ring species interpretation. *Syst Biol*, 41, 273–291.
- Nei, M., Maruyama, T. & Wu, C.I. (1983). Models of evolution of reproductive isolation. *Genetics*, 103, 557–579.
- Nuismer, S. & Doebeli, M. (2004). Genetic correlations and the coevolutionary dynamics of three-species systems. *Evolution*, 58, 1165–1177.
- Nuismer, S.L., Jordano, P. & Bascompte, J. (2012). Coevolution and the architecture of mutualistic networks. *Evolution*, 67, 338–354.
- Ohta, T. (2002). Near-neutrality in evolution of genes and gene regulation. *Proc Natl Acad Sci USA*, 99, 16134–16137.

Okuyama, T. & Holland, J.N. (2008). Network structural properties mediate the stability of mutualistic communities. *Ecol. Lett.*, 11, 208–216.

Olesen, J., Bascompte, J., Dupont, Y., Elberling, H., Rasmussen, C. & Jordano, P. (2010). Missing and forbidden links in mutualistic networks. *Proc. R. Soc. Lond. B.*

Olesen, J. & Jordano, P. (2002). Geographic patterns in plant-pollinator mutualistic networks. *Ecology*, 89, 2416–2424.

Olesen, J.M., Bascompte, J., Elberling, H. & Jordano, P. (2008). Temporal dynamics in a pollination network. *Ecology*, 89, 1573–1582.

Paradis, E., Claude, J. & Strimmer, K. (2004). Ape: analyses of phylogenetics and evolution in R language. *Bioinformatics*, 20, 289–290.

Pérez, F. & Granger, B. (2007). IPython: a System for Interactive Scientific Computing. *Comput. Sci. Eng.*, 9, 21–29.

R Core Team (2013). *R: A Language and Environment for Statistical Computing*. R Foundation for Statistical Computing, Vienna, Austria.

Rainey, P. & Travisano, M. (1998). Adaptive radiation in a heterogeneous environment. *Nature*, 394, 69–72.

Rambaut, A. & Grassly, N. (1997). Seq-gen: An application for the monte carlo simulation of dna sequence evolution along phylogenetic trees. *Computer Applications In The Biosciences*, 13, 235–238.

Rezende, E.L., Jordano, P. & Bascompte, J. (2007). Effects of phenotypic complementarity and phylogeny on the nested structure of mutualistic networks. *Oikos*, 116, 1919–1929.

Santamaría, L. & Rodríguez-Gironés, M.A. (2007). Linkage rules for plant-pollinator networks: trait complementarity or exploitation barriers? *PLoS Biol*, 5, e31.

Schluter, D. (2009). Evidence for ecological speciation and its alternative. *Science*, 323, 737–741.

705 Seehausen, O., Butlin, R.K., Keller, I., Wagner, C.E., Boughman, J.W., Hohenlohe, P.A., Peichel,
706 C.L., Saetre, G.P. *et al.* (2014). Genomics and the origin of species. *Nature Reviews Genetics*, 15,
707 176–192.

708 Servedio, M., Kopp, G.V.M., Frame, A. & Nosil, P. (2011). Magic traits in speciation: 'magic' but
709 not rare? *Trends Ecol Evol*, 26, 389–399.

710 Solé, R., Ferrer-Cancho, R., Montoya, J. & Valverde, S. (2002). Selection, tinkering, and emergence
711 in complex networks. *Complexity*, 8, 20–33.

712 Stang, M., Klinkhamer, P. & van der Meijden, E. (2006). Size constraints and flower abundance
713 determine the number of interactions in a plant-flower visitor web. *Oikos*, 112, 111–121.

714 Stang, M., Klinkhamer, P., Waser, N., Stang, I. & van der Meijden, E. (2009). Size-specific interaction
715 patterns and size matching in a plant-pollinator interaction web. *Ann Bot*, 103, 1459–1469.

716 Stayton, C.T. (2008). Is convergence surprising? An examination of the frequency of convergence in
717 simulated datasets. *J. Theo. Biol.*, 252, 1–14.

718 Thibert-Plante, X. & Gavrillets, S. (2013). Evolution of mate choice and the so-called magic traits
719 in ecological speciation. *Ecology letters*, 16, 1004–1013.

720 Thompson, J.N. (1999). Specific hypotheses on the geographic mosaic of coevolution. *The American*
721 *Naturalist*, 153, S1–S14.

722 Thompson, J.N. (2009). The coevolving web of life. *The American Naturalist*, 173, 125–140.

723 Thompson, J.N. & Cunningham, B.M. (2002). Geographic structure and dynamics of coevolutionary
724 selection. *Nature*, 417, 735–738.

725 True, J.R. & Haag, E.S. (2001). Developmental system drift and flexibility in evolutionary trajec-
726 tories. *Evolution & Development*, 3, 109–119.

727 van Doorn, G. & Weissing, F. (2001). Ecological versus sexual models of sympatric speciation: a
728 synthesis. *Selection*, 2, 17–40.

- 729 Vellend, M. (2010). Conceptual synthesis in community ecology. *The Quarterly Review of Biology*,
730 85, 183–206.
- 731 Wagner, A. (2008). Neutralism and selectionism: a network-based reconciliation. *Nature Reviews*
732 *Genetics*, 9, 965–974.
- 733 Waser, N., Chittka, L., Price, M., Williams, N. & Ollerton, J. (1996). Generalization in pollination
734 systems, and why it matters. *Ecology*, 77, 1043–1060.
- 735 Welch, J.J. (2004). Accumulating Dobzhansky-Muller incompatibilities: Reconciling theory and
736 data. *Evolution*, 58, 1145–1156.

Table 1: Glossary of mathematical notation and parameter values

Notation	Definition	Values
J^P, J^A	Effective population size of plants (P) and animals (A)	1,000
d_{ij}^P, d_{ij}^A	Geographical pairwise distance plants (P) and animals (A)	variable
d_{max}	Maximum geographical distance to mate and disperse	0.3
D^P, D^A	Geographic distance matrix with all d_{ij}^P and d_{ij}^A values	variable
d_{ik}^{PA}	Geographical distance between plant i and animal k	variable
d_{max}^{PA}	Maximum geographical distance to find a mutualistic partner	0.3
D^{PA}	Geographic distance matrix with all the d_{ik}^{PA} values	variable
q_{ij}^P, q_{ij}^A	Genetic similarity between ind. i and j in (P) and (A)	variable
Q^P, Q^A	Genetic similarity matrix with all the q_{ij}^P and q_{ij}^A values	variable
q_{min}	Minimum genetic similarity to have viable offspring	0.97
z_i^P, z_i^A	Quantitative trait of ind. i in (P) and (A)	variable
Z^P, Z^A	Quantitative trait distribution in (P) and (A)	variable
p_{ij}^P, p_{ij}^A	Phenotypic similarity between ind. i and j in (P) and (A)	variable
$\mathcal{P}^P, \mathcal{P}^A$	Phenotypic similarity matrix with all the p_{ij}^P and p_{ij}^A values	variable
L	Size of the genome	150
g_i^P, g_i^A	Genetic component of phenotype of offspring in (P) and (A)	variable
ϵ	Environmental component of phenotype of offspring	$\mathcal{N}(0,1)$
μ	Mutation rate per locus	$10^{-4} - 10^{-2}$
$\hat{q}_{kh}^P, \hat{q}_{kh}^A$	Mean genetic simil. between species k and h in (P) and (A)	variable
Q_s^P, Q_s^A	Species genetic simil. matrix with all \hat{q}_{kl}^P and \hat{q}_{kl}^A values	variable
$\hat{p}_{kh}^P, \hat{p}_{kh}^A$	Mean phen. simil. between species k and h in (P) and (A)	variable
$\mathcal{P}_s^P, \mathcal{P}_s^A$	Species phen. simil. matrix with all \hat{p}_{kl}^P and \hat{p}_{kl}^A values	variable
\hat{p}_{kh}^{PA}	Mean trait similarity plant species k and animal species h	variable
\mathcal{P}_s^{PA}	Phenotypic simil. matrix with all \hat{p}_{kh} values	variable

Table 2: Predictions of the model and observed values in real mutualistic webs. Overall, qualitative predictions are very similar to observed ecological and evolutionary patterns. However, quantitatively we find many differences in the network topology, trait distribution and evolutionary patterns.

	<i>Model predictions</i>	<i>Real webs</i>
<i>Nestedness</i>	Highly nested	Highly nested (Bascompte <i>et al.</i> , 2006)
<i>Connectance</i>	Medium connectance (0.5)	Low to medium connectance (0.01-0.38) (Olesen & Bascompte, 2005)
Bimodal or multimodal trait distribution	Log-normal distribution (right-skewed) (Stang <i>et al.</i> , 2009)	
<i>Convergence</i>	Low to medium convergence (17 %)	High levels of convergence (Bascompte & Jordano, 2007)
<i>Complementarity</i>	Low to medium complementarity (20 %)	High levels of complementarity (Rezende <i>et al.</i> , 2007)
<i>Diversity</i>	Highly diverse (using low population size ~1000 indiv)	Highly diverse (Bronstein <i>et al.</i> , 2001)

Figures

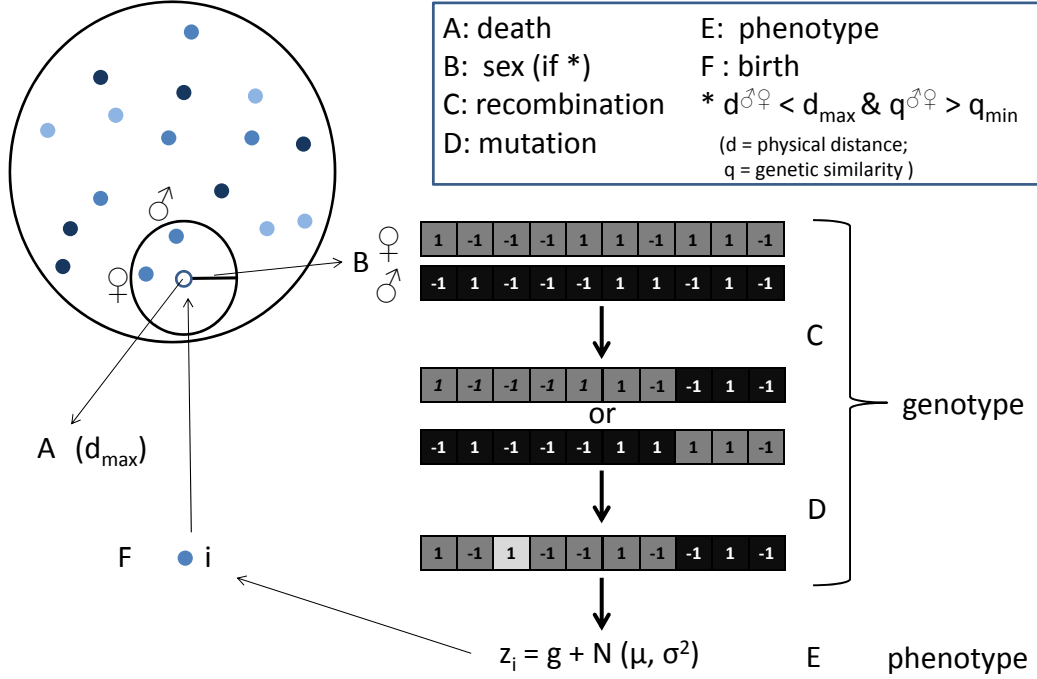


Figure 1: This figure summarizes the death-birth cycle per time step. Individuals are represented as filled circles and blue tones represent variation of phenotypes. (A) an individual k is randomly selected to die and leaves an empty location in the landscape. (B) a female individual, φ , is randomly selected among all females satisfying the condition $d_{k\varphi}^{\sigma\varphi} < d_{max}$. We then choose randomly a male, σ , among all males satisfying $d_{k\sigma}^{\sigma\varphi} < d_{max}$ and $q_{\varphi\sigma}^{\sigma\varphi} > q_{min}$ with q_{min} , the minimum genetic similarity required for mating. In addition to these two constraints, two more are required to complete mating. For the condition of obligate mutualism, the geographic distance between the female (animal or plant), and an animal (or plant) individual j , must satisfy $d_{j\varphi}^{PA} < d_{max}^{PA}$. Finally, female plants need the presence of an animal pollinator with a larger or equally-sized proboscis than the corolla of the female plant, thus individual pollinators represented as j , must satisfy $z_{\varphi_P} \leq z_{j_A}$. In (C) and (D) we calculate the genome of the new offspring once these constraints are satisfied. (C) Genomes are composed of L loci where each locus can be in two allelic states ($-1, 1$) and undergo block crossover recombination between female (dark gray) and male (black). A position l in the genome of the parents is randomly chosen partitioning the genome in two blocks. All genes beyond the l locus in either organism's genome is swapped between two parents and two new genomes are formed. (D) One of the two new genomes is randomly chosen for the offspring i , S_o^i , and it might undergo mutation (light gray). (E) The phenotype expression of offspring i is $z_i = g_i + \epsilon$ with $g_i = L + S_o^i$ and ϵ are the genetic and environmental component of the phenotype, respectively. (F) The offspring i occupies the site of the dead individual k .

Q_s matrix

	a	b	c
a		0.85	0.97
b			0.89
c			

P_s matrix

	a	b	c
a		0.98	0.90
b			0.92
c			

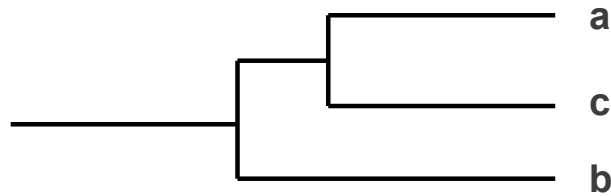


Figure 2: This figure illustrates a simple example of evolutionary convergence using species a , b and c . The upper matrix ($Q_S = [\hat{q}_{kl}]$) shows species a and c are genetically closely related, $\hat{q}_{ac} = 0.97$, while genetically distant from species b ($\hat{q}_{ab} = 0.85$, $\hat{q}_{cb} = 0.89$). A clear description of these genetic relationships can be represented with a cluster tree or dendrogram, as shown in the lower part of the figure. Thus, we establish that species a and c are sister species. The species phenotypic similarity matrix, $P_S = [\hat{p}_{kh}]$ shows that species a and b are phenotypically highly similar ($\hat{p}_{ab} = 0.98$) and highly genetically dissimilar ($\hat{q}_{ab} = 0.85$) (i.e. more than the average intraspecific genetic similarity or sister species 0.97), indicating an event of evolutionary convergence.

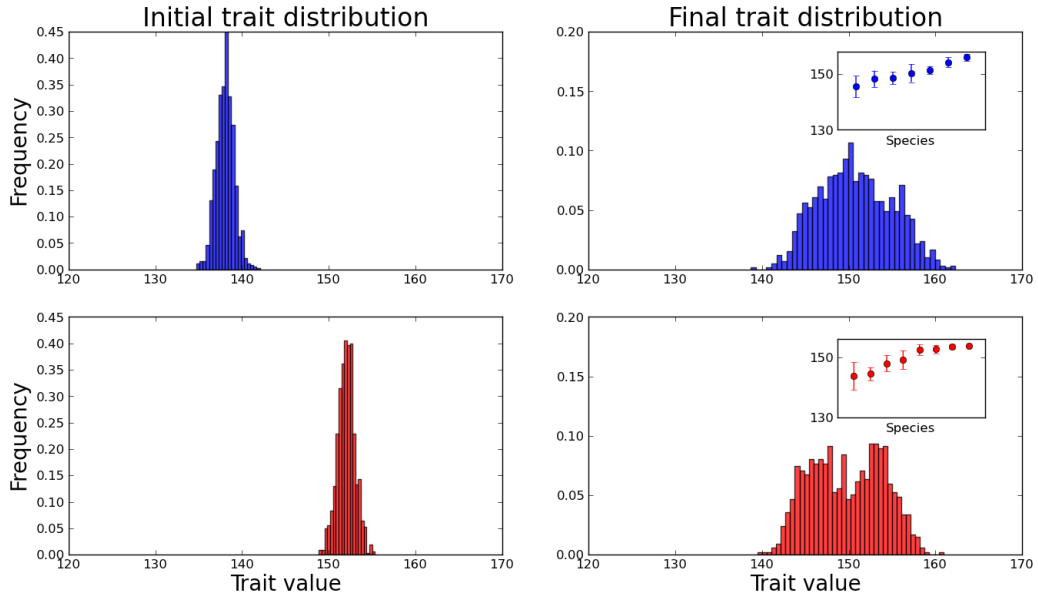


Figure 3: Changes in trait distribution of plants (top, blue) and animals (bottom, red). Left and right panels show the initial and final trait distribution, respectively. The insets in the right panels show the mean trait and standard error for each species sorted from the most common to the most rare. Initial trait distributions changed towards higher variance, and in most replicates, towards bimodal distribution in both guilds. Plot shows the outputs from one replicate with parameters values $q_{min} = 0.97$, $d_{max} = d_{max}^{PA} = 0.3$, $\mu = 5 \times 10^{-3}$ and $J_P = J_A = 1,000$.

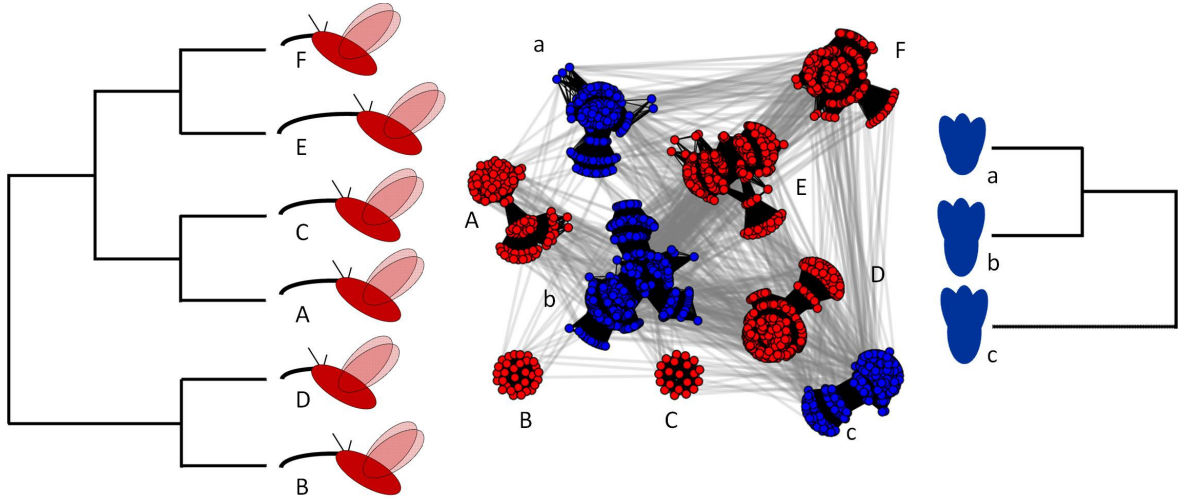


Figure 4: Evolutionary convergence and complementarity in plant-pollinator networks. Trees at the left and right side show genetic similarities between animal (red) and plant (blue) species, respectively. Mean species trait, proboscis and corolla length, is sketched with cartoons next to their respective position in the trees. Animals, composed by six species, have two evolutionary convergence events (A-B and F-D). Plants, composed by three species, have one convergent event (b-c). The central part of the figure shows the network of plant-animal interactions, where each node (colored filled circles) represents an individual. The network is composed of two types of links: genetic relatedness links (black solid) forming clusters that represent species and plant-animal individual-based interaction links (gray). The network shows variability in terms of genetic relatedness and plant-animal interactions within a species (i.e. high intraspecific variability). This figure is an example from one replicate simulation. Parameters used are as in figure 3, $q_{min} = 0.97$, $d_{max} = d_{max}^{PA} = 0.3$, $\mu = 5 \times 10^{-3}$ **and** $J^P = J^A = 1,000$.

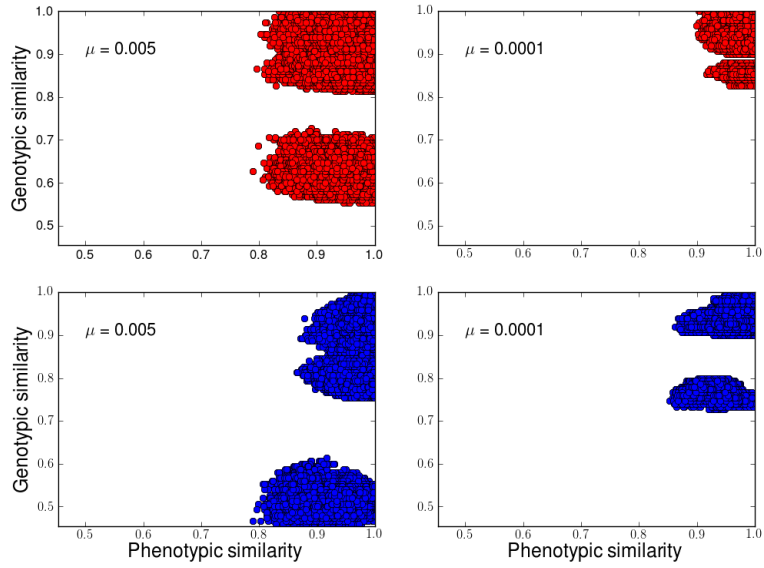


Figure 5: The effect of mutation rate on the genotype-phenotype relationship. Top and bottom panels show the genotype-phenotype relationship for animals (red) and plants (blue), respectively. Right panels show the genotype-phenotype relationship for mutation rate $\mu = 5 \times 10^{-3}$ and left panels for $\mu = 10^{-4}$. Each plot is a scatter plot, where each filled circle represents phenotypic and genetic similarity between two individuals of a particular guild (plant or animal) from one replicate. Individuals with high phenotypic similarity and genetic dissimilarity suggests evolutionary convergence of traits, regardless of mutation rate. Parameters used are $q_{min} = 0.97$, $d_{max} = d_{max}^{PA} = 0.3$ and $J_P = J_A = 1,000$.

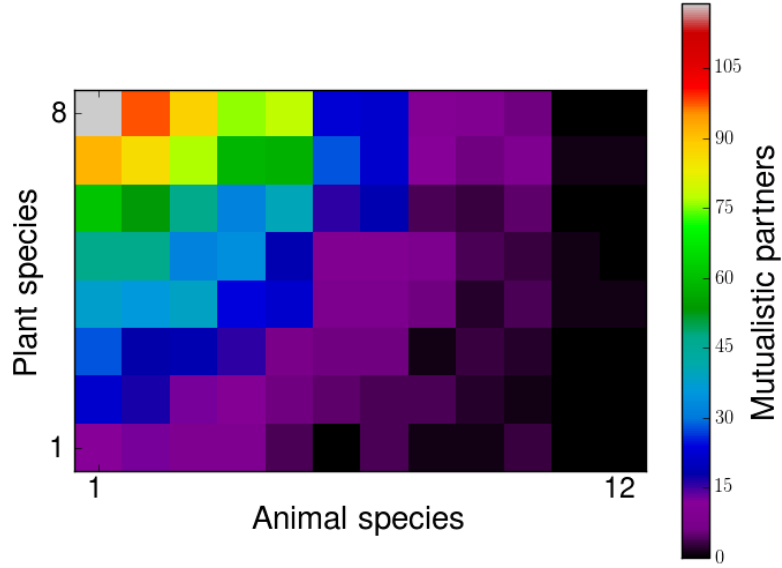


Figure 6: Plant-animal species interaction network. Plant species are represented in rows and animal species in columns. The color gradient indicates the number of mutualistic partners (i.e. individuals interacting) shared between plant and animal species. This matrix comes from one replicate with nine plant and thirteen animal species. The network shows high level of nestedness ($N = 0.72$) and intermediate level of connectance ($C = 0.5$). Parameters used are $q_{min} = 0.97$, $d_{max} = d_{max}^{PA} = 0.3$, $\mu = 5 \times 10^{-3}$ and $J_P = J_A = 1,000$.

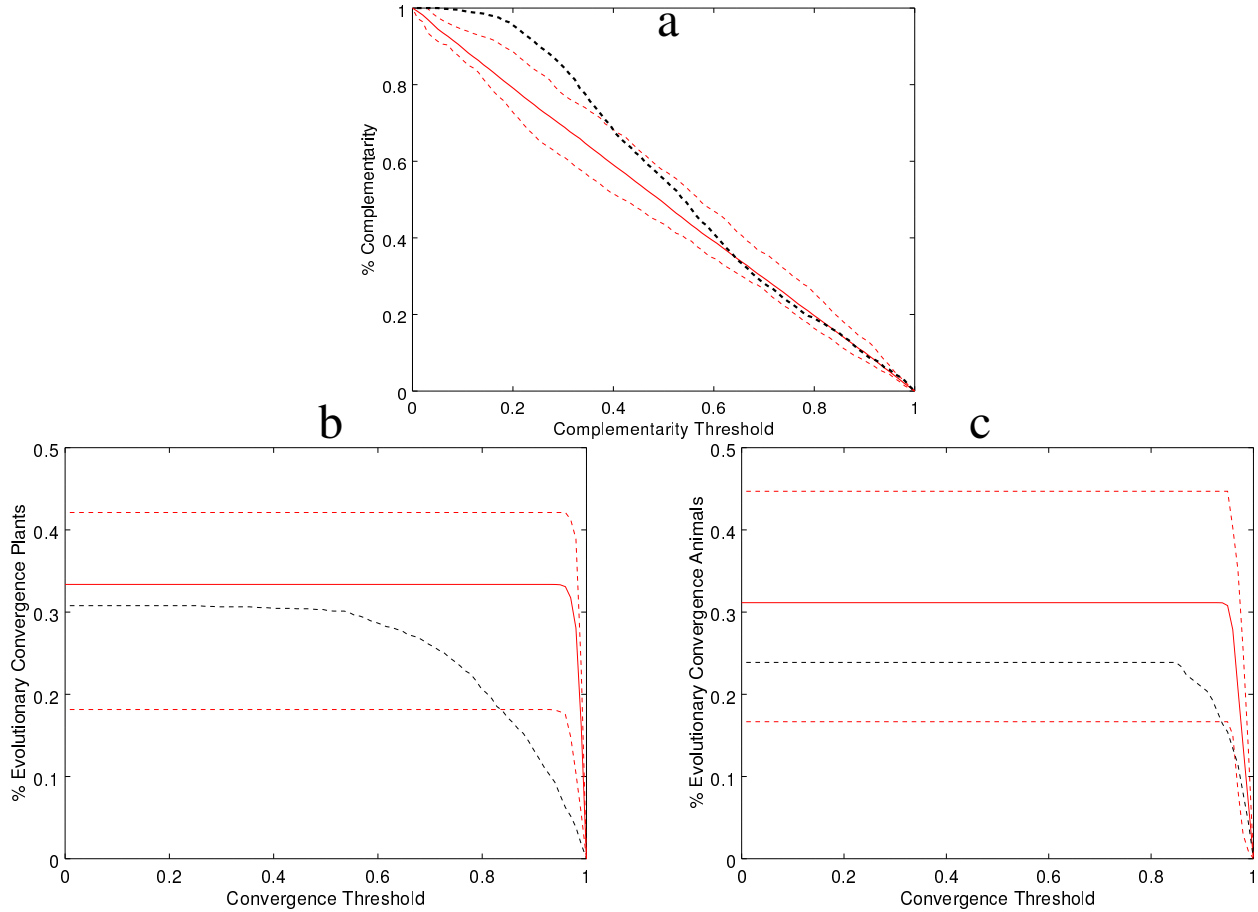


Figure 7: Comparison of model's predictions with estimations of convergence and complementarity from an empirical data of a plant-pollinator community. a) Shows the proportion of complementarity events (y-axis) as a function of the complementarity threshold (x-axis) for the empirical data (dotted black line) and for the model (continuous and dotted lines represent mean and CI values, respectively). Predictions are within the CI for most complementarity threshold values. Empirical data deviates from model predictions for complementarity values around 0.4 and lower. b) Shows the proportion of convergence events in the plant community (y-axis, 69 species) as a function of the convergence threshold (x-axis) for the empirical data (dotted black line) and for the model (continuous and dotted lines represent mean and CI values, respectively). Convergence events in the empirical data strongly deviates from model predictions for convergence threshold values ranging between 1 and 0.82. In that range, model predicts much faster proportion of convergence events than the empirical observations. c) Shows the proportion of convergence events in the animal community (y-axis, 24 species) as a function of the convergence threshold (x-axis) for the empirical data (dotted black line) and for the model (continuous and dotted lines represent mean and CI values, respectively). Convergence events in the empirical data are within the CI of model predictions for most convergence threshold values.